

- <sup>4</sup>D. C. Golibersuch and A. J. Heeger, Phys. Rev. **182**, 584 (1969); Solid State Commun. **8**, 17 (1970).
- <sup>5</sup>M. D. Daybell and W. A. Steyert, Phys. Rev. Letters **18**, 398 (1967); C. M. Hurd, J. Phys. Chem. Solids **28**, 1345 (1967).
- <sup>6</sup>J. L. Tholence and R. Tournier, Phys. Rev. Letters **25**, 867 (1970).
- <sup>7</sup>J. E. Potts and L. B. Welsh, Phys. Letters **34A**, 397 (1971).
- <sup>8</sup>L. B. Welsh and J. E. Potts, Phys. Rev. Letters **26**, 1320 (1971).
- <sup>9</sup>A. Narath, in *Progress in Low Temperature Physics*, edited by C. J. Gorter (North-Holland, Amsterdam, 1970), Vol. 12.
- <sup>10</sup>D. C. Golibersuch, thesis (University of Pennsylvania, 1969) (unpublished).
- <sup>11</sup>P. M. Chaikin and M. A. Jensen, Solid State Commun. **8**, 977 (1970).
- <sup>12</sup>W. W. Simmons, W. J. O'Sullivan, and W. A. Robinson, Phys. Rev. **127**, 1168 (1962); A. Narath, *ibid.* **162**, 320 (1967).
- <sup>13</sup>O. J. Lumpkin, Phys. Rev. **164**, 324 (1967); R. E. Levine, Phys. Letters **28A**, 504 (1969).
- <sup>14</sup>M. Hanabusa and T. Kushida (unpublished).
- <sup>15</sup>G. Gladstone, J. Appl. Phys. **41**, 1150 (1970).
- <sup>16</sup>L. B. Welsh, A. J. Heeger, and M. A. Jensen, J. Appl. Phys. **39**, 696 (1968).
- <sup>17</sup>B. Caroli, J. Phys. Chem. Solids **28**, 1427 (1967).
- <sup>18</sup>A. Blandin, in *Proceedings of the Enrico Fermi School of Physics, Course 37* (Academic, New York, 1967).
- <sup>19</sup>A. Narath and A. C. Gossard, Phys. Rev. **183**, 391 (1969).
- <sup>20</sup>L. Bennett, R. W. Mebbs, and R. E. Watson, Phys. Rev. **171**, 611 (1968).
- <sup>21</sup>J. Applebaum and J. Kondo, Phys. Rev. Letters **19**, 906 (1967); Phys. Rev. **170**, 542 (1968).
- <sup>22</sup>P. E. Bloomfield, R. Hecht, and P. Sievert, Phys. Rev. B **2**, 3714 (1970).
- <sup>23</sup>A. Narath, K. C. Brog, and W. H. Jones, Jr., Phys. Rev. B **2**, 2618 (1970).
- <sup>24</sup>B. Giovanninni, P. Pincus, G. Gladstone, and A. J. Heeger, J. Phys. (Paris) **32**, C1-163 (1971).
- <sup>25</sup>H. Benoit, P. G. de Gennes, and D. Silhouette, Compt. Rend. **256**, 3841 (1963), referred to as BGS.
- <sup>26</sup>B. Giovanninni and A. J. Heeger, Solid State Commun. **7**, 287 (1969).
- <sup>27</sup>M. R. McHenry, B. G. Silbernagel, and J. H. Wernick, Phys. Rev. Letters **27**, 426 (1971); M. R. McHenry, thesis (University of California, Santa Barbara, 1971) (unpublished).
- <sup>28</sup>H. Nagasawa and W. A. Steyert, J. Phys. Soc. Japan **28**, 1202 (1970).
- <sup>29</sup>G. Gladstone, thesis (University of Pennsylvania, 1970) (unpublished).
- <sup>30</sup>J. E. Potts, thesis (Northwestern University, 1971) (unpublished).

## Nuclear-Magnetic-Resonance Study of Tightly Pinned Domain Walls in $\alpha\text{-Fe}_2\text{O}_3$

C. W. Searle, S. Kupca, and J. H. Davis

*Department of Physics, University of Manitoba, Winnipeg, Manitoba, Canada*

(Received 6 December 1971)

$\text{Fe}^{57}$  NMR in  $\alpha\text{-Fe}_2\text{O}_3$  is used to determine the behavior of tightly pinned domains in a static magnetic field. The predominant positive-phase component of the NMR signal is found to be due to strongly pinned domains with  $\sim 180^\circ$  antiferromagnetic walls. A model wherein domains are nucleated about local-strain axes is proposed to explain the observed behavior. Finally, a possible explanation of the anomalous temperature dependence of the spontaneous moment reported by Searle and Dean is suggested.

### INTRODUCTION

Hematite is basically an antiferromagnet with a weak spontaneous moment which appears because of a slight canting of the sublattice magnetizations toward one another via the Dzialoshinski-Moriya canting interaction and, therefore, some interesting domain configurations might be expected. A domain structure was first detected in hematite by Blackman *et al.*,<sup>1</sup> and since this time several workers have tried to establish exactly what type of domain structure is present in this material.<sup>2-6</sup> The various techniques that have been used to this end include neutron diffraction, the Faraday effect, and the Bitter technique.

Recent nuclear-magnetic-resonance (NMR) studies by Hirai *et al.*<sup>7</sup> suggest that the NMR signals in  $\alpha\text{-Fe}_2\text{O}_3$  originate in domain walls. This observation has been put on strong experimental grounds by Maartense and Searle,<sup>8</sup> who directly detected a domain-wall resonance predicted by Hirai *et al.*<sup>7</sup>

The nuclear-resonance frequency for an individual nucleus depends on the projection of the applied field  $\vec{H}_0$  on the direction of the hyperfine field  $\vec{H}_{\text{hf}}$  at the nucleus, as long as  $|\vec{H}_0| \ll |\vec{H}_{\text{hf}}|$ . The angular distribution of  $\vec{H}_{\text{hf}}$  with respect to  $\vec{H}_0$  through the domain wall is expected to be sensitive to the wall structure. Thus, since the NMR signals originate in domain walls, the behavior of the

line shape and intensity should be a sensitive probe of the domain-wall structure.

Accordingly, a reexamination of the  $\text{Fe}^{57}$  NMR in hematite was performed with particular interest in observing the changes in line shape with applied field. The experimental methods and some of the crystals used have already been described by Hirai *et al.*<sup>7</sup>

### EXPERIMENTAL RESULTS

Figure 1 illustrates the change in the NMR line shape with  $\vec{H}_0$ . In this case the rf field  $\vec{h}_{\text{rf}}$  is parallel to  $\vec{H}_0$  and both fields are applied in the basal plane. In this configuration, for small  $\vec{H}_0$ , as reported previously,<sup>7</sup> two types of signals with opposite phases are observed. The negative signal is associated with mobile or easily moved walls, while the positive signal arises from what have been termed "pinned" walls, i. e., domain walls which are not easily removed by application of  $\vec{H}_0$ . When  $\vec{H}_0$  is applied, the negative component of the signal disappears at such small values of field that the structure of the mobile walls could not be examined by NMR. However, a detailed study of this type of wall has been performed by Eaton and Morrish<sup>6</sup> using the Bitter technique. The best available information on the strongly pinned walls has been the neutron-diffraction data of Nathans *et al.*<sup>4</sup> Fortunately, the strongly pinned walls are not removed by small fields and can be studied quite directly using the present technique. From Fig. 1 it is seen that the signal broadens appreciably with increasing  $\vec{H}_0$ , with an indication of two distinct peaks shifted symmetrically above and below  $\nu_0$ , the  $H_0 = 0$  resonant frequency. This type of behavior was observed in all the crystals examined: two pure synthetic crystals from different runs and one natural crystal of unknown origin.

Figures 2(a) and 2(b) show the NMR lines for  $\vec{h}_{\text{rf}} \perp \vec{H}_0$  and  $\vec{h}_{\text{rf}} \parallel \vec{H}_0$ , respectively. The fields were applied in the basal plane in both cases, and  $\vec{H}_0$  was small enough so that the mobile walls were not re-

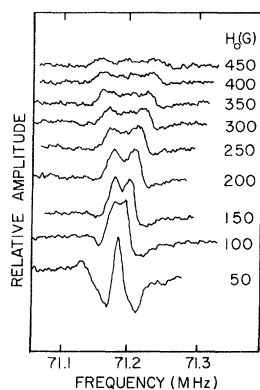


FIG. 1. Dependence of NMR line shape on applied field.

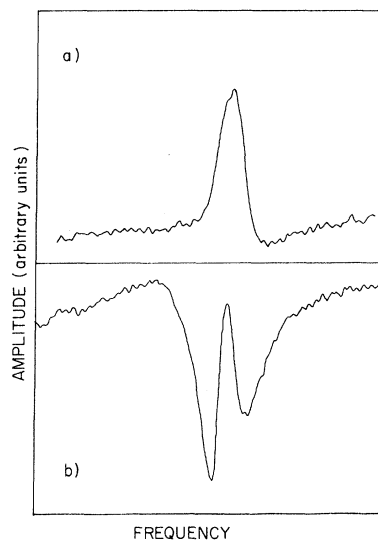


FIG. 2. NMR signal intensity for small  $H_0$  in basal plane (a)  $\vec{H}_0 \perp \vec{h}_{\text{rf}}$  and (b)  $\vec{H}_0 \parallel \vec{h}_{\text{rf}}$  [amplitude of (a)  $\sim \frac{1}{3}$  amplitude of (b)].

moved. As shown in Fig. 2(a),  $\vec{h}_{\text{rf}} \perp \vec{H}_0$  does not excite the nuclei in the mobile walls. We also note that the signal intensity associated with the pinned walls has decreased.

The total linewidth  $\Delta\nu_T$ , defined as the distance between half-peak points, is plotted against  $H_0$  in Fig. 3.  $\Delta\nu_T$  is not well defined for small values of  $H_0$  where there is a mixture of two signals with opposite phases; this is the reason no experimental point is plotted for  $H_0 = 0$ . As  $H_0$  increases the phase associated with the mobile walls is quickly removed (see Fig. 1) and  $\Delta\nu_T$  becomes well defined. The linewidth as shown does not appear to be related to any field-dependent loss process but rather seems to be related to a distribution of resonant frequencies which broadens with increasing  $H_0$ . In fact, this effect is expected since the signals originate in domain walls, for, if the domain walls are  $180^\circ$  antiferromagnetic (AF) walls, then  $\Delta\nu_T$  should be of the form

$$\Delta\nu_T = \Delta\nu(H_0) + \Delta\nu_n = (2\gamma_N/2\pi)H_0 + \Delta\nu_n, \quad (1)$$

where  $\gamma_N$  is the nuclear gyromagnetic ratio for  $\text{Fe}^{57}$  and  $\Delta\nu_n$  is the natural linewidth in zero field. This follows for  $180^\circ$  AF walls since there will always be some nuclei in the wall whose  $\vec{H}_{\text{wf}}$ 's are parallel and some whose  $\vec{H}_{\text{wf}}$ 's are antiparallel to  $\vec{H}_0$ . These two extremes provide the upper and lower bounds for the distribution of resonant frequencies and lead directly to Eq. (1), which is represented by the dashed curve appearing in Fig. 3.

Figure 4 shows the field-induced linewidth evaluated at 1 kG as a function of  $\alpha$ , the angle between  $\vec{H}_0$  and the [111] direction. The experimental points were obtained using the slopes of curves such as

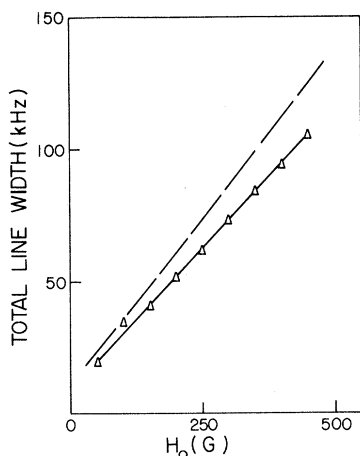


FIG. 3. Total linewidth  $\Delta\nu_T$  vs applied field. The dashed line is from Eq. (1).

that shown in Fig. 3. If the spins are confined to the basal plane, then the effective field leading to  $\Delta\nu(H_0)$  is the component of  $\vec{H}_0$  in the basal plane, or,  $\Delta\nu(H_0)$  as a function of  $\alpha$  can be expressed as

$$\Delta\nu(H_0) = (2\gamma_N/2\pi)H_0 \sin\alpha. \quad (2)$$

Equation (2) is the solid curve which appears in Fig. 4 and approximately describes the experimental data. The error bars on the data are the result of obtaining the slopes from lines such as that shown in Fig. 3, and do not include any error associated with crystal alignment. Although there was always an experimental  $\Delta\nu(H_0)$  at  $\alpha = 0$ , which implied an angle of inclination out of the basal plane on the order of  $(2-3)^\circ$ , when the experimental error of crystal alignment is considered one must come to the conclusion that the spins are confined to the

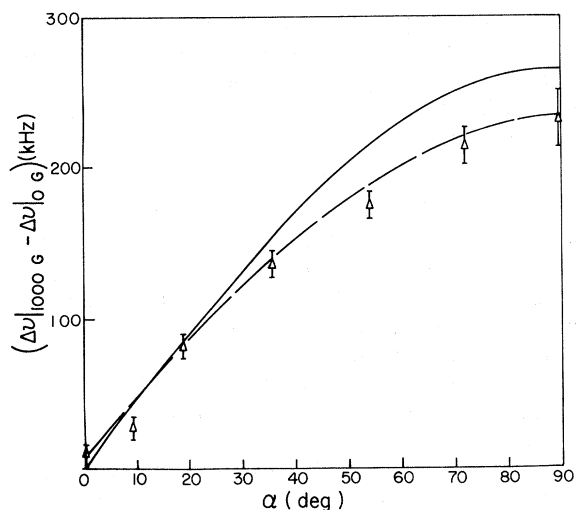


FIG. 4. Angular dependence of field-induced linewidth at 1 kG.

basal plane within an error of  $\sim \pm 3^\circ$ .

#### DISCUSSION OF RESULTS

As an illustration of a tightly pinned domain we consider a strain which, as depicted in Fig. 5, induces a local uniaxial anisotropy whose axis is at some angle to  $\vec{H}_0$ . There is expected to be a random distribution in direction of these strain axes throughout the crystal. If, as in Fig. 5, we give the antiferromagnetic axis a sense (i. e., a direction) then the solid lines of Fig. 5 represent the antiferromagnetic axes in the direction of the open arrowhead in a region near a strongly pinned domain. Figure 5(a) then represents a strongly pinned domain in the absence of external field  $\vec{H}_0$ . For small  $\vec{H}_0$ , Fig. 5(b), there will be a slight rotation of the pinned moment  $\vec{m}$  and a slight decrease in the size of the domain, but there will always be some spins in the domain wall which are parallel and some which are antiparallel to  $\vec{H}_0$ , as required by Eq. (1). As the magnitude of  $\vec{H}_0$  is increased, the domain's moment  $\vec{m}$  will change direction until for some large  $\vec{H}_0$  we have the situation in Fig. 5(c), where  $\vec{m}$  is aligned nearly parallel to  $\vec{H}_0$ , and the pinned domain has become essentially a ripple in the magnetization near the strain.

The shape of the lines shown in Fig. 1 indicates that the domains involved have nearly  $180^\circ$  AF walls with approximately a linear relation between  $\theta$ , the

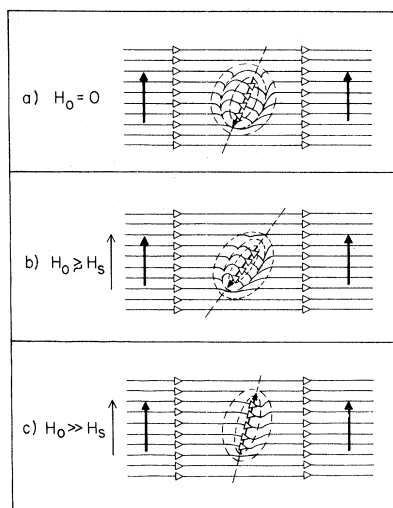


FIG. 5. Tightly pinned domain.  $H_s$  is the saturation field for easily movable domains. The heavy solid arrows represent the magnetization of the bulk material and the light solid arrows represent the magnetization of the tightly pinned domain. The unbroken horizontal lines represent the antiferromagnetic axis in the basal plane and the open arrowheads represent the direction of a sublattice magnetization vector. The dashed curves represent the approximate spatial extent of the tightly pinned domain wall.

angle between the individual spin axes and  $\vec{H}_0$  (for small  $H_0$ ), and the distance into the domain wall. The projection of  $\vec{H}_0$  on the local spin axis then varies with distance into the domain wall as  $\cos\theta$ . Therefore, since  $\cos\theta$  is much more rapidly varying near  $\theta = \pi/2$  than at  $\theta = 0$  or  $\pi$ , the spins near the "center" of the domain wall, which have a resonance splitting  $\delta\nu = \gamma_N/2\pi H_0$ , will contribute the largest component of the NMR signal. Thus, for the model shown in Fig. 5, the application of  $\vec{H}_0$  leads to a distribution of resonant frequencies having maxima near  $\delta\nu = \pm \gamma_N/2\pi H_0$  and thus to the two distinct peaks shown in Fig. 1.

It has already been pointed out that the data shown in Fig. 4 indicate that the nuclear spins in the domain walls are confined to the basal plane to within  $\sim 3^\circ$ . The anomalous temperature dependence of  $M_0$ , the weak magnetic moment, reported by Searle and Dean<sup>9</sup> is therefore not related to a large temperature-dependent inclination of the antiferromagnetic axis, or to a simple splitting of the two-sublattice structure into a four-sublattice structure as they suggest, unless the behavior of the spins in the domain walls is considerably different from that of spins in the bulk material. This is in agreement with the observation of Levinson,<sup>10</sup> who used Mössbauer data to conclude that the spins were confined to the basal plane to within an experimental error of  $10^\circ$ , although his intensity data (uncorrected for sample thickness) suggest a large angle of inclination or a splitting of sublattices amounting to  $\sim 18^\circ$ .

In any case, the NMR data presented here reveal the presence of  $\sim 180^\circ$  AF domain walls which are surprisingly difficult to remove and, as has been pointed out, extremely large  $\vec{H}_0$  would yield a uniform  $\vec{M}$  with a superimposed ripple near a strain center as depicted in Fig. 5(c). The net result will be apparent high-field differential susceptibilities as given in Eq. (3):

$$\begin{aligned}\chi_{(111)} &= \chi_r + \frac{1}{\lambda}, \\ \chi_{[111]} &= \frac{1}{\lambda},\end{aligned}\quad (3)$$

where  $\lambda$  is the molecular-field constant and  $\chi_r$  is the contribution to the susceptibility associated with a gradual reduction of the rippling in  $\vec{M}$  with increasing  $H_0$ . Equation (3) predicts that

$$\chi_{(111)} > \chi_{[111]}. \quad (4)$$

This was checked by measuring  $\chi_{(111)}$  and  $\chi_{[111]}$  for five different samples and it was found that the inequality given by relation (4) was always satisfied with  $\chi_{(111)}$  being on the average 4% greater than  $\chi_{[111]}$ . Equation (3) also points out that any linear extrapolation to obtain the weak spontaneous moment  $M_0$  will underestimate it if the applied fields are not large enough to eliminate  $\chi_r$ . This effect

TABLE I.  $T = 295^\circ\text{K}$ .

Sample preparation	$H'_D$ (kG)
quenched	$19.7 \pm 0.2$
as grown	$20.2 \pm 0.2$
annealed	$20.4 \pm 0.2$
annealed <sup>a</sup>	$22.0 \pm 0.6$

<sup>a</sup> $H'_D$  obtained from ferromagnetic resonance (Ref. 11).

could be the origin of the anomalous temperature dependence of  $M_0$  reported by Searle and Dean.<sup>9</sup>

This possibility was explored further by measuring  $H'_D$ , the apparent canting field, using the following relation:

$$H'_D = M_0 / \chi_{(111)}, \quad (5)$$

where  $M_0$  is the extrapolated  $H_0 = 0$  value for the weak magnetic moment and  $\chi_{(111)}$  is the high-field differential susceptibility.

It was found that  $M(H_0)$  apparently saturated for  $H_0 > 5$  kG and was quite linear between 5 and 18 kG (the largest field available). Thus all of our experimental values of  $M_0$  and  $\chi_{(111)}$  were obtained using experimental data obtained for  $18 > H_0 > 5$  kG.  $H'_D$  was the experimental quantity examined since an important source of experimental error, the calibration constant for the vibrating sample magnetometer, cancels out as can be seen in Eq. (5). The results of the experiment are indicated in Table I.  $H'_D$  determined from ferromagnetic resonance is included in Table I, since for the following reasons it is expected to be the best value for  $H'_D$ .

In a ferromagnetic-resonance (FMR) experiment the  $k=0$ , or uniform precessional mode, is excited. The uniform precession is influenced by all of the strain centers which lead to  $\chi_r$ ; however, since the effective fields associated with the strain centers are oriented randomly, the average total effective field acting on the uniform mode tends to zero. Therefore,  $H'_D$  obtained from FMR should be more free of the influence of strains than  $H'_D$  obtained using static measurements.

An examination of Table I indicates that  $H'_D$  increases when strain centers are removed. This is consistent with our model as seen in Eq. (4), since  $M_0$  increases and  $\chi_{(111)}$  decreases with the removal of strains. This behavior was confirmed by repeating the experiment on another crystal. The fact that  $H'_D$  obtained from the most well-annealed sample is less than that obtained from ferromagnetic resonance is also consistent with the NMR data, since all attempts at annealing reduced the number of strain centers but did not completely remove all of them. This is because the strength of the NMR signal associated with the strongly pinned domains was reduced with annealing but never completely eliminated.

## CONCLUSIONS

NMR studies can yield information on the dynamics of domain walls in materials where the signals arise from nuclei within domain walls.<sup>7</sup> In addition, it has been shown that an NMR study can be used to study the static arrangement of spins within a domain wall somewhat quantitatively. In particular, it has been found that the strongly pinned

domains in hematite having approximately 180° AF walls (which are difficult to remove with an applied field) are responsible for the largest contribution to the positive-phase NMR signal.

The experimental data also suggest that the anomalous temperature dependence of  $M(T)$  may be related to these strongly pinned walls. It is suggested that careful magnetization measurements in extremely large fields might clear up this point.

<sup>1</sup>M. Blackman, G. Haigh, and N. D. Lisgarten, *Nature* **179**, 1288 (1957).

<sup>2</sup>H. J. Williams, R. C. Sherwood, and J. P. Remeika, *J. Appl. Phys.* **29**, 1772 (1958).

<sup>3</sup>M. Blackman and B. Gustard, *Nature* **193**, 360 (1962); also, in *Proceedings of the International Conference on Magnetism, Nottingham*, 1964 (The Institute of Physics and The Physical Society, London 1965), p. 600.

<sup>4</sup>R. Nathans, S. J. Pickart, H. A. Alperin, and P. J. Brown, *Phys. Rev.* **136**, A1641 (1964).

<sup>5</sup>T. E. Gallon, *Proc. Roy. Soc. (London)* **A303**, 511

(1958).

<sup>6</sup>J. A. Eaton and A. H. Morrish, *J. Appl. Phys.* **40**, 3180 (1969).

<sup>7</sup>A. Hirai, J. A. Eaton, and C. W. Searle, *Phys. Rev. B* **3**, 68 (1971).

<sup>8</sup>I. Maartense and C. W. Searle, *J. Appl. Phys.* **42**, 2349 (1971).

<sup>9</sup>C. W. Searle and G. W. Dean, *Phys. Rev. B* **1**, 4337 (1970).

<sup>10</sup>Lionel M. Levinson, *Phys. Rev. B* **3**, 3965 (1971).

<sup>11</sup>A. H. Morrish and C. W. Searle, in Ref. 3, p. 574.

## Calculation of Isomer Shift in Mössbauer Spectroscopy\*

B. Fricke and J. T. Waber

*Department of Materials Science, Northwestern University, Evanston, Illinois 60201*

(Received 12 November 1971)

The approximations normally used in the calculation of the isomer shift are compared with the exact expressions using Dirac-Slater orbitals and a three-parameter Fermi-type nuclear charge distribution. The nonuniformity of the electronic density over the nuclear volume affects the results. Different choices of the nuclear surface thickness  $t$  and the radius  $c$  in the protonic density  $\rho_N(r)$  also affects the isomer shift differently even though the values are chosen to yield a given value of  $\Delta\langle r^2 \rangle$ . The change in the electronic charge density which is caused by the alteration of  $\rho_N(r)$  in the ground state and excited state of the nucleus is discussed using two extreme models and the possible influence on the observable isomer shift is estimated.

The Coulomb interaction energy between the charge distribution of the electrons  $\rho_e(r)$  in an atom and the charge distribution of the protons  $\rho_N(r')$  in the nucleus is given in first-order perturbation theory by the expression

$$-e^2 \iint \rho_N(\vec{r}') \rho_e(\vec{r}) \frac{1}{|\vec{r} - \vec{r}'|} d\tau' d\tau. \quad (1)$$

The usual multipole expansion, in terms of spherical harmonics  $Y_{lm}$ , gives rise to the monopole interaction energy

$$-e^2 \iint \frac{\rho_N(r') \rho_e(r)}{r_{>}} d\tau' d\tau, \quad (2)$$

where  $r_{>}$  is the larger of  $r$  and  $r'$ . This term with

$l=0$  can be used to calculate the isomer shift whereas  $l=2$  leads to the electric quadrupole interaction. Both terms can be measured in Mössbauer spectroscopy. A number of review articles have appeared<sup>1-6</sup> on the isomer shift which deal with the increasing number of experimental results and with improved theoretical understanding. Our purpose is to discuss here the approximations used in the literature and compare them with the results obtained with the mathematically exact expressions.

The isomer shift in Mössbauer spectroscopy is nonzero when two changes occur: (a) when the nuclear charge distribution of the excited state  $\rho_N^*(r')$  and the ground state  $\rho_N(r')$  are different, and (b) when the electronic charge distribution inside the nucleus in the source  $\rho_e^s(r)$  and in the absorber  $\rho_e^A(r)$  are different. So the expression for the isomer shift becomes